



---

**Título artículo / Títol article:** A Fast and Precise Method To Identify Indolic Glucosinolates and Camalexin in Plants by Combining Mass Spectrometric and Biological Information

**Autores / Autors** Sara Izquierdo Zandalinas, Vicente Vives-Peris, Aurelio Gómez-Cadenas, Vicent Arbona

**Revista:** Journal of Agricultural and Food Chemistry, 2012, 60 (35)

**Versión / Versió:** Postprint del autor

**Cita bibliográfica / Cita bibliogràfica (ISO 690):** IZQUIERDO ZANDALIAS, Sara; VIVES-PERIS, Vicente; GÓMEZ-CADENAS, Aurelio; ARBONA, Vicent. A Fast and Precise Method To Identify Indolic Glucosinolates and Camalexin in Plants by Combining Mass Spectrometric and Biological Information. *Journal of Agricultural and Food Chemistry*, 2012, vol. 60, no 35, p. 8648-8658.

**url Repositori UJI:** <http://hdl.handle.net/10234/62572>

---

# A Fast and Precise Method To Identify Indolic Glucosinolates and Camalexin in Plants by Combining Mass Spectrometric and Biological Information

Sara Izquierdo Zandalinas, Vicente Vives-Peris, Aurelio Gómez-Cadenas, and Vicent Arbona\*

Departament de Ciències Agràries i del Medi Natural, Universitat Jaume I, Campus de Riu Sec. Avda, Sos Baynat s/n, E-12071 Castelló de la Plana, Spain

**S** Supporting Information

**ABSTRACT:** In this manuscript, a fast and accurate identification and quantitation by mass spectrometry of indolic glucosinolates and camalexin involved in defense in *Arabidopsis thaliana* are described. Two elicitation systems, inoculation with *Botrytis cinerea* and treatment with AgNO<sub>3</sub>, were used in Col-0 wild-type and mutant genotypes impaired in the biosynthesis of the selected metabolites. Identification of analytes was carried out by nontargeted LC/ESI-QTOF-MS profiling. Confirmation of indolic glucosinolates and camalexin was achieved by their absence in the *cyp79B2/B3* and *pad3* mutants as well as their respective fragmentation upon collision-induced dissociation. Camalexin accumulation was induced only after AgNO<sub>3</sub> treatment, whereas all indolic glucosinolates were constitutively present. Inoculation with *Botrytis* did not influence camalexin concentration but caused most aliphatic and indolic glucosinolates contents to decrease. Only the *pen 3.1* mutant showed increased indolic glucosinolate levels after *Botrytis* or AgNO<sub>3</sub> treatments. In addition, profiles of secondary metabolite in nontreated Col-0 and mutant plants were analyzed by means of partial least squares coupled to discriminant analysis (PLS-DA), and differences in the basal levels of indolic glucosinolates and tryptophan between *cyp79B2/B3* plants and the rest of genotypes, including Col-0, were found. This probably has to be taken into consideration when comparing stress responses of Col-0 and *cyp79B2/B3*. The use of mutants carrying alterations in biosynthetic pathways is proposed as a useful strategy to identify secondary metabolites.

**KEYWORDS:** metabolomics, LC/ESI-QTOF-MS, abiotic stress, biotic stress, secondary metabolism, phytoalexins

## INTRODUCTION

In response to environmental stress conditions, plants activate a plethora of responses including changes in growth and developmental patterns and primarily severe alterations in metabolic processes such as glycolysis, tricarboxylic acid cycle, and aminoacid biosynthesis.<sup>1,2</sup> Abiotic stress conditions, such as drought or salinity, directly affect carbon assimilation and consequently alter plant primary metabolism.<sup>2,3</sup> It has been shown that the stress conditions also affect the accumulation of different minor compounds with a less clear interconnection with photosynthesis.<sup>4,5</sup> These compounds, collectively referred to as secondary metabolites, are of very diverse origins, and their composition and biosynthesis are not yet well understood. Their biological roles are also very diverse and include antioxidant properties, defense, or signaling.<sup>6–8</sup> Interestingly, they are specific for given species or botanical families. Therefore, these compounds could be used as markers to certify plant material from different origins,<sup>9</sup> an important aspect when dealing with many species of importance to human nutrition and health.

Among all edible plants, Brassicaceae is the botanical family including more species important in agriculture and human nutrition, for example, cabbage, turnip, rapeseed, etc. Glucosinolates, the most abundant compounds of this family, are sulfur- and nitrogen-containing molecules that carry a hydroxyaminosulfate group and  $\beta$ -thioglucosyl residue attached to a variable side chain.<sup>10</sup>

Glucosinolates are synthesized from aminoacids by conversion to the respective acetaldoxime derivative by cytochromes (CYP79F1/F2 and CYP79B2/B3, Figure 1, adapted from ref 11). Depending on the side chain, glucosinolates can be divided into aliphatic (derived from alanine, methionine, valine, or leucine), aromatic (derived from tyrosine or phenylalanine), and indolic (which are mainly derived from tryptophan).<sup>11,12</sup> These compounds have been primarily associated with defense against biotic stressors such as herbivores, fungi, and also bacteria acting as growth deterrents or as powerful toxic substances. To exert their biological activity, the  $\beta$ -thioglucosyl residue needs to be cleaved by a specific enzyme known as myrosinase, a type of thioglycosidase. This enzyme cleaves the  $\beta$ -thioglucosidic bond, yielding mainly isothiocyanates, thiocyanates, and nitriles, which are responsible for the biological activity of glucosinolates.<sup>12,13</sup>

Among all known glucosinolates (more than 120 structures characterized so far), the indolics are the most important involved in stress defense.<sup>12–14</sup> In the model plant species, *Arabidopsis thaliana*, these metabolites are derived from tryptophan after cleavage with a CYP79 enzyme that converts the precursor tryptophan to indole-3-acetaldoxime. This metabolite is the primary precursor of both indolic

**Received:** June 7, 2012

**Revised:** August 6, 2012

**Accepted:** August 8, 2012

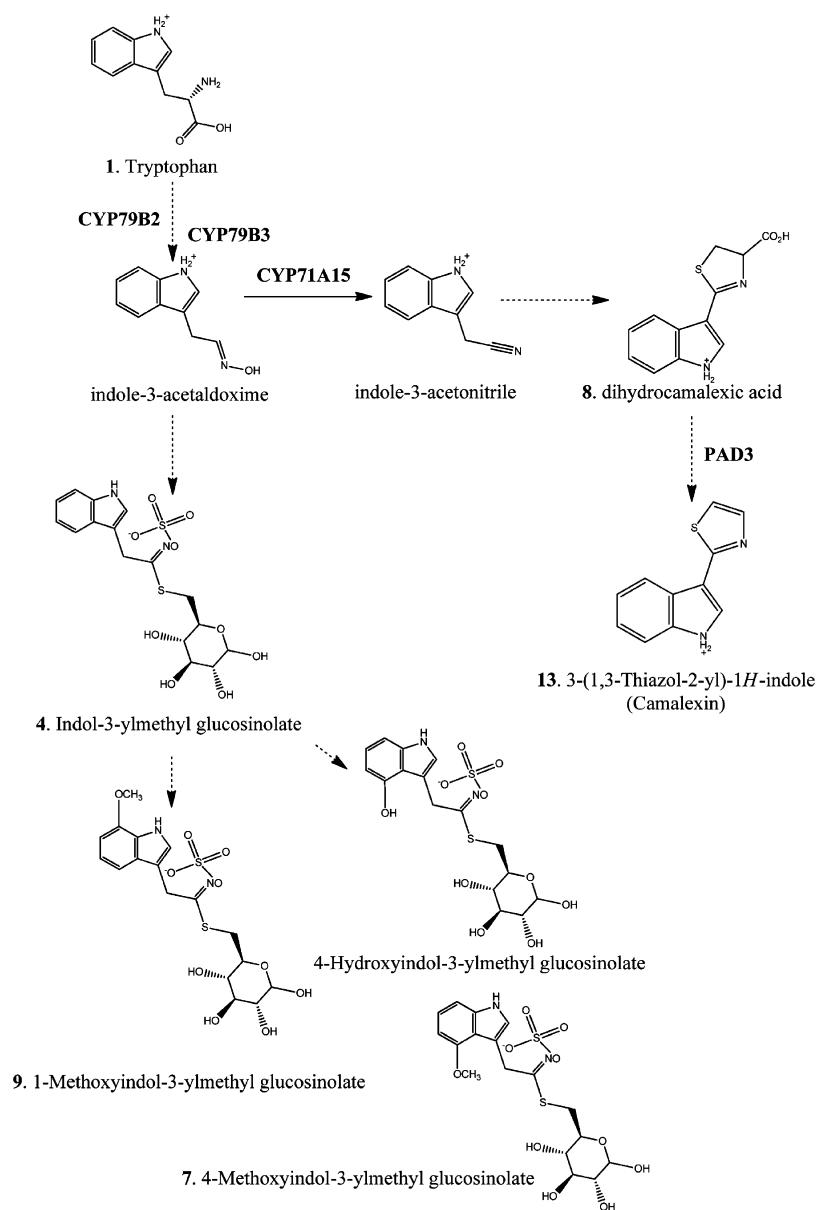


**Figure 1.** Metabolic pathway of indolic glucosinolates with names of key biosynthetic steps highlighted. The compounds detected in the profiles are indicated in Arabic numerals. The scheme was adapted from ref 11.

72 glucosinolates and camalexin [3-(1,3-thiazol-2-yl)-1H-indole],  
 73 the main phytoalexin. Indolic glucosinolates are always present  
 74 in plant tissues, although their relative levels might change  
 75 depending on the specific genetic background, tissue or  
 76 developmental stage,<sup>14</sup> and in response to environmental  
 77 cues.<sup>14,15</sup> On the contrary, phytoalexins are only produced  
 78 under certain stress conditions, such as pathogen elicitation,  
 79 heavy metal toxicity, etc.<sup>6</sup> In this sense, it is likely that the  
 80 production of glucosinolates in *A. thaliana* under certain stress  
 81 conditions is tightly regulated.<sup>16,17</sup>

82 Stress responses might reflect whole plant performance,  
 83 physiological status, or even a genetic modification. Therefore,  
 84 there is an increasing demand for high-throughput methods to  
 85 evaluate slight variations in minor compounds.<sup>4,9</sup> In this sense,  
 86 LC/MS-based metabolite profiling techniques provide an  
 87 unbiased methodology for the analysis of semipolar com-  
 88 pounds.<sup>9,18</sup> Current metabolite profiling platforms take  
 89 advantage of modern mass spectrometers (as well as other

powerful techniques, such as NMR) to gather molecular 90  
 information on metabolites to aid in structural elucidation and 91  
 identification. However, mass spectrometry is not enough to 92  
 identify all metabolites present in a given sample, and it 93  
 becomes necessary to coinject reference standards, which are 94  
 not always commercially available. In addition, in the analysis of 95  
 intact glucosinolates, it is crucial to first suppress all myrosinase 96  
 activity by boiling the samples to prevent cleavage to take 97  
 place.<sup>19</sup> 98

In metabolite profiling techniques, a bottleneck is the 99  
 identification of metabolites. In high-resolution mass spectrom- 100  
 etry, such as hybrid quadrupole time-of-flight (QTOF), 101  
 identification of metabolites starts by formulating a hypothesis 102  
 on the identity of a metabolite based on the ion composition of 103  
 the mass chromatographic feature, search of informative 104  
 fragmentations, and calculation of elemental composition. 105  
 However, the unbiased identification of a certain metabolite 106  
 is limited to the commercial availability of analytical stand- 107

108 ards.<sup>18</sup> This is of special relevance in the case of indolic  
109 glucosinolates, for which no commercial standards are  
110 available.<sup>19</sup> To overcome this problem, a set of *Arabidopsis*  
111 mutants lacking different key enzymes in indolic glucosinolate  
112 or camalexin biosynthesis were included in this study. In  
113 addition, two different adverse conditions were assayed: biotic  
114 stress by inoculating plants with *Botrytis cinerea* conidia, a  
115 necrotrophic fungal plant pathogen to which *A. thaliana* has  
116 developed a nonhost resistance,<sup>20</sup> and abiotic stress by spraying  
117 plants with a AgNO<sub>3</sub> solution, which induces the accumulation  
118 of camalexin.<sup>20,21</sup>

119 In this work, the main objective was to unequivocally identify  
120 indolic glucosinolates and camalexin in *Arabidopsis* plants by  
121 using the biological information obtained from mutants  
122 impaired in the biosynthesis of these compounds. In addition,  
123 the impact of biotic and abiotic stress on glucosinolate and  
124 camalexin accumulation and the difference in metabolite  
125 composition among *Arabidopsis* mutants and wild-type plants  
126 were analyzed.

## 127 ■ MATERIALS AND METHODS

128 **Reagents and Standards.** Liquid chromatography–mass spec-  
129 trometry (LC-MS) grade acetonitrile from Panreac (Barcelona, Spain)  
130 and Milli-Q water (Millipore Corp., Billerica, MA) were used for the  
131 liquid chromatography/electrospray ionization–quadrupole time-of-  
132 flight mass spectrometry (LC/ESI-QTOF-MS) analyses. Formic acid  
133 (Panreac) was used as the mobile phase modifier. For extractions,  
134 methanol (MeOH LC-MS grade) from Panreac was used. Biochanin A  
135 (5,7-dihydroxy-4'-methoxyisoflavone) and leucine-enkephalin were  
136 obtained from Sigma-Aldrich (Madrid, Spain). For stress treatments  
137 and *Botrytis* culture, AgNO<sub>3</sub> and KH<sub>2</sub>PO<sub>4</sub> were purchased from  
138 Panreac.

139 **Plant Cultivation and Stress Treatments.** Plant material used in  
140 the experiments was *A. thaliana* accessions Col-0 as wild type and  
141 mutants *pad3*,<sup>22,23</sup> *cyp79B2/B3*,<sup>24</sup> and *pen3.1*,<sup>20</sup> all in the Col-0  
142 background. Seeds were germinated in jiffy pellets (Jiffy Products  
143 España S.L.U., Murcia, Spain) and allowed to grow for 2 weeks in a  
144 growth chamber with 8 h of illumination at 21 °C and 16 h of darkness  
145 at 18 °C. After that time, seedlings were transplanted to individual jiffy  
146 pellets and allowed to grow for 6 more weeks before imposition of  
147 treatments. For abiotic and biotic stress treatments, plants were  
148 sprayed with a 5 mM AgNO<sub>3</sub> solution or with a *B. cinerea* conidia  
149 suspension (5 × 10<sup>4</sup> conidia/mL in Gamborg medium, supplemented  
150 with 10 μmol/L sucrose and KH<sub>2</sub>PO<sub>4</sub>, as described in ref 25). Control  
151 plants were sprayed with tap water. After 24 h of each treatment, leaf  
152 rosettes of the different genotypes were harvested, immediately frozen  
153 in liquid nitrogen, ground to fine powder, and stored at –80 °C until  
154 analysis. Two independent biological replicate experiments were  
155 performed, and three independent sample replicates per sample group  
156 and experiment were analyzed by LC/ESI-QTOF-MS.

157 **Extraction.** Extraction was performed essentially as previously  
158 described in ref 19 with slight modifications. Briefly, 500 μL of 70%  
159 methanol supplemented with biochanin A at 1 mg/L (internal  
160 standard, IS) was added to 0.1 g of frozen leaf powder. After 10 min of  
161 sonication, samples were incubated for 15 min at 80 °C in a water bath  
162 to stop myrosinase activity. Extracts were allowed to cool down at  
163 room temperature and centrifuged at 10000g for 10 min at 4 °C. Prior  
164 to UPLC-QTOF-MS analysis, supernatants were filtered through 0.2  
165 μm PTFE syringe filters (Whatman International Inc., Kent, United  
166 Kingdom).

167 **Instrumentation and Conditions.** Chromatographic separations  
168 were performed on an Acquity SDS system (Waters Corp. Ltd.,  
169 Milford, MA) interfaced to a QTOF Premier from Micromass Ltd.  
170 through an ESI source. Two reversed-phase columns were evaluated as  
171 follows: 100 mm × 2.1 mm i.d., 5 μm, XTerra C18 LC-MS (Waters),  
172 and 100 mm × 2.1 mm i.d., 2.1 μm, ProntoSIL C18SH (Bischoff  
173 Chromatography, Leonberg, Germany). Samples were injected in the

UPLC system in 10 μL aliquots using the partial loop-filling option. 174  
Separations were carried out using two gradients at a flow rate of 300 175  
μL/min. Conditions of gradient 1 were as follows: 0–2 min, isocratic 176  
95% A [water:formic acid, 99.9:0.1 (v/v)] and 5% B [acetonitrile:- 177  
formic acid, 99.9:0.1 (v/v)]; 2–27 min, gradient 5–95% B; 27–30 178  
min, return to initial conditions; 30–35 min, re-equilibration period. 179  
Conditions of gradient 2 were as follows: 0–2 min, isocratic 5% B; 2– 180  
17 min, gradient 5–95% B; 17–20 min, return to initial conditions; 181  
20–25 min, re-equilibration period. During analyses, the column 182  
temperature was maintained at 40 °C, and samples were maintained at 183  
5 °C to slow down degradation. 184

Samples were analyzed in both negative and positive ionization 185  
modes. Two functions were set in the instrument: in function 1, data 186  
were acquired in profile mode from 50 to 1000 Da using a scan time of 187  
0.2 s and a collision energy of 2 eV; in function 2, the scan range was 188  
the same, but a collision ramp between 4 and 65 eV was set. During all 189  
measurements, the electrospray capillary voltage was set to 4 kV, and 190  
the cone voltage was set to 25 V. The source temperature was 191  
maintained at 120 °C, and the desolvation gas temperature was set at 192  
350 °C. Argon was used as the collision gas, and nitrogen was used as 193  
the nebulizer as well as desolvation gas set at 60 and 800 L/h, 194  
respectively. Exact mass measurements were provided by monitoring 195  
the reference compound lockmass leucine-enkephalin. 196

**Data Processing.** Data were processed using Masslynx v.4.1. Raw 197  
data files were converted to netCDF format using the application 198  
*databridge* from Masslynx and processed using the *xcms* package.<sup>26</sup> 199  
Chromatographic peak detection was performed using the match- 200  
edFilter algorithm,<sup>27</sup> applying the following parameter settings: snr = 3, 201  
fwhm = 15 s, step = 0.01 D, mzdiff = 0.1 D, and profmethod = bin. 202  
Retention time correction was achieved in three iterations applying the 203  
parameter settings minfrac = 1, bw = 30 s, mzwid = 0.05 D, span = 1, 204  
and missing = extra = 1 for the first iteration; minfrac = 1, bw = 10 s, 205  
mzwid = 0.05 D, span = 0.6, and missing = extra = 0 for the second 206  
iteration; and minfrac = 1, bw = 5 s, mzwid = 0.05 D, span = 0.5, and 207  
missing = extra = 0 for the third iteration. After final peak grouping 208  
(minfrac = 1, bw = 5 s) and filling in of missing features using the 209  
fillPeaks routine of the *xcms* package, a data matrix consisting on 210  
feature × sample was obtained. In these data sets, only consistent mass 211  
signals were considered, whose significance level of *P* values (*t* test, 212  
two-tailed, unequal variances) was lower than 0.05. 213

Data mean comparisons were performed with Statgraphics Plus 214  
V.5.1. software (Statistical Graphics Corp., Herndon, VA). One-way 215  
analysis of variance (ANOVA) was performed to assess differences 216  
between treatments and genotypes considering a significance value of 217  
0.05. Posthoc data mean comparisons were achieved with a least 218  
significant difference (LSD) test. For multivariate analysis of the whole 219  
data set, peak detection and retention time correction of control 220  
samples of each genotype were performed using a similar set of 221  
parameters as described above. After filling in missing chromato- 222  
graphic mass features and removal of inconsistent features, principal 223  
component analysis (PCA) and partial least-squares discriminant 224  
analysis (PLS-DA) were performed using Simca-P (v 11.0) software 225  
(Umetrics, Umea, Sweden). 226

## 227 ■ RESULTS AND DISCUSSION

**Optimization of Chromatography.** Until now, few 228  
studies have described the use of UPLC-MS for the analysis 229  
of glucosinolates and camalexin. Recently, a new powerful 230  
identification tool has become available: the hybrid QTOF 231  
mass spectrometer. In addition to the improved characteristics 232  
of TOF instruments, they offer the possibility of performing 233  
MS/MS acquisitions to obtain product ion spectra with 234  
accurate mass, which is sometimes necessary to aid in the 235  
identification of compounds or even differentiate between 236  
structural isomers.<sup>22,27</sup> 237

In this first part of this work, the objective was to develop a 238  
nontargeted metabolite profiling methodology for the analysis 239  
of variations in indolic glucosinolate and camalexin levels in *A. thaliana* 240

Table 1. List of Metabolites Identified in *Arabidopsis* Leaf Extracts<sup>a</sup>

no.	compd name	formula	quantifier ion type, m/z	R <sub>t</sub> (min)	pseudomolecular ion			CID fragmentation <sup>b</sup>
					ion type	theor m/z	exptl m/z	
1	tryptophan	C <sub>11</sub> H <sub>12</sub> N <sub>2</sub> O <sub>2</sub>	[M + H] <sup>+</sup> 205.09	4.03	[M + H] <sup>+</sup>	205.0977	205.0997	<b>205</b> , 188, 146, 118, 91
					[M - H] <sup>-</sup>	203.08205	203.0774	<b>203</b> , 142, 116, 74
2	4-methylthiobutyl glucosinolate	C <sub>12</sub> H <sub>23</sub> NO <sub>9</sub> S <sub>3</sub>	[M - H] <sup>-</sup> 420.05	3.89	[M + K] <sup>+</sup>	460.0172	460.0112	<b>460</b> , 342, 238, 192
					[M - H] <sup>-</sup>	420.0456	420.0459	<b>420</b> , 259, 178, 96
3	7-methylsulfinylheptyl glucosinolate	C <sub>15</sub> H <sub>29</sub> NO <sub>10</sub> S <sub>3</sub>	[M - H] <sup>-</sup> 478.09	3.87	[M + K] <sup>+</sup>	518.05906	518.0777	<b>518</b> , 298
					[M - H] <sup>-</sup>	478.08753	478.0866	<b>478</b> , 259, 96
4	indol-3-ylmethyl glucosinolate	C <sub>16</sub> H <sub>18</sub> N <sub>2</sub> O <sub>9</sub> S <sub>2</sub>	[M - H] <sup>-</sup> 447.06	4.41	—	—	—	—
					[M - H] <sup>-</sup>	447.05319	447.0525	<b>447</b> , 96
5	8-methylsulfinyloctyl glucosinolate	C <sub>16</sub> H <sub>31</sub> NO <sub>10</sub> S <sub>3</sub>	[M - H] <sup>-</sup> 492.10	4.74	[M + Na] <sup>+</sup>	516.10077	516.094	<b>516</b> , 414, 252, 96
					[M - H] <sup>-</sup>	492.10318	492.1010	<b>492</b> , 428, 96
6	5-methylthiopentyl glucosinolate	C <sub>13</sub> H <sub>25</sub> NO <sub>9</sub> S <sub>3</sub>	[M - H] <sup>-</sup> 434.06	5.01	—	—	—	—
					[M - H] <sup>-</sup>	434.06132	434.0618	<b>434</b> , 96
7	4-methoxyindol-3-ylmethyl glucosinolate	C <sub>17</sub> H <sub>22</sub> N <sub>2</sub> O <sub>10</sub> S <sub>2</sub>	[M - H] <sup>-</sup> 477.06	5.21	[M + K] <sup>+</sup>	517.03529	517.0386	<b>517</b> , 479, 437, 399, 237, 160
					[M - H] <sup>-</sup>	477.06376	477.0606	<b>477</b> , 96
8	dihydrocamalexin acid	C <sub>12</sub> H <sub>10</sub> N <sub>2</sub> O <sub>2</sub> S	[M + H] <sup>+</sup> 247.05	5.59	[M + H] <sup>+</sup>	247.05412	247.0605	<b>247</b> , 201, 143, 118
					—	—	—	—
9	1-methoxyindol-3-ylmethyl glucosinolate	C <sub>17</sub> H <sub>22</sub> N <sub>2</sub> O <sub>10</sub> S <sub>2</sub>	[M - H] <sup>-</sup> 477.06	5.91	[M + H] <sup>+</sup>	479.07941	479.0876	<b>479</b> , 437, 399, 237, 160
					[M - H] <sup>-</sup>	477.06376	477.0629	<b>477</b> , 44, 96
10	unknown aliphatic glucosinolate*	C <sub>14</sub> H <sub>26</sub> NO <sub>9</sub> S <sub>2</sub>	[M - H] <sup>-</sup> 416.10	6.60	—	—	—	—
					[M - H] <sup>-</sup>	416.10489	416.1093	<b>416</b> , 389, 357, 323, 119, 96
11	7-methylthioheptyl glucosinolate	C <sub>15</sub> H <sub>29</sub> NO <sub>9</sub> S <sub>3</sub>	[M - H] <sup>-</sup> 462.09	6.76	—	—	—	—
					[M - H] <sup>-</sup>	462.09261	462.0941	<b>462</b> , 96
12	8-methylthiooctyl glucosinolate	C <sub>16</sub> H <sub>31</sub> NO <sub>9</sub> S <sub>3</sub>	[M - H] <sup>-</sup> 476.11	7.55	[M + H] <sup>+</sup>	478.12391	478.1278	<b>478</b> , 398, 236
					[M - H] <sup>-</sup>	476.10826	476.1089	<b>476</b> , 96
13	3-(1,3-thiazol-2-yl)-1H-indole (camalexin)	C <sub>11</sub> H <sub>8</sub> N <sub>2</sub> S	[M + H] <sup>+</sup> 201.05	8.91	[M + H] <sup>+</sup>	201.04864	201.0517	<b>201</b> , 174, 160, 142, 59
					[M - H] <sup>-</sup>	199.03299	199.0321	<b>199</b> , 158, 141, 130
14	5,7-dihydroxy-4'-methoxy-isoflavone (biochanin A)**	C <sub>16</sub> H <sub>12</sub> O <sub>5</sub>	[M + H] <sup>+</sup> 285.07	10.93	[M + H] <sup>+</sup>	285.07629	285.0773	<b>285</b> , 270, 242, 213, 152, 124
					[M - H] <sup>-</sup>	283.06065	283.0594	<b>283</b> , 268, 239, 211, 132

<sup>a</sup>Note: dashes (—) denote missing ions, or when expected, pseudomolecular ions or adducts could not be identified. Rt, retention time; \*, tentative annotation; and \*\*, internal standard. <sup>b</sup>Numbers in bold represent precursor ions.

241 *thaliana*. Therefore, it had to be possible to unequivocally  
 242 identify these metabolites in plant extracts. As reported  
 243 previously,<sup>18</sup> reversed phase liquid chromatography is the best  
 244 suited technique for the analysis of secondary metabolites in  
 245 *Arabidopsis*. In this project, two C18 columns were assayed, a  
 246 XTerra C18 and a ProntoSIL C18SH. Samples of stressed *A.*  
 247 *thaliana* plants were analyzed in triplicate by using also two  
 248 gradients. As expected, the XTerra column tested with either  
 249 gradient 1 or gradient 2 gave worse resolution than ProntoSIL  
 250 C18SH due to the higher particle size, although all considered  
 251 metabolites could be detected. Using gradient 2, the total  
 252 chromatographic run took about 20 min, and all glucosinolates

and camalexin eluted in less than 11 min, and using gradient 1, 253  
 the total chromatographic run took 30 min, and the metabolites 254  
 of interest eluted within 15 min. 255

After the chromatographic analysis, peaks were extracted and 256  
 aligned using xcms software. The number of peaks obtained 257  
 was taken as an estimate of the performance of the column. In 258  
 both cases, samples analyzed with the ProntoSIL C18SH 259  
 column rendered a higher number of aligned mass features than 260  
 the same samples analyzed with XTerra C18 LC-MS. The use 261  
 of the short gradient implied losing 12.2 and 5.3% of the total 262  
 peaks in positive and negative mode, respectively. This was 263  
 considered acceptable taking into consideration the time (10 264



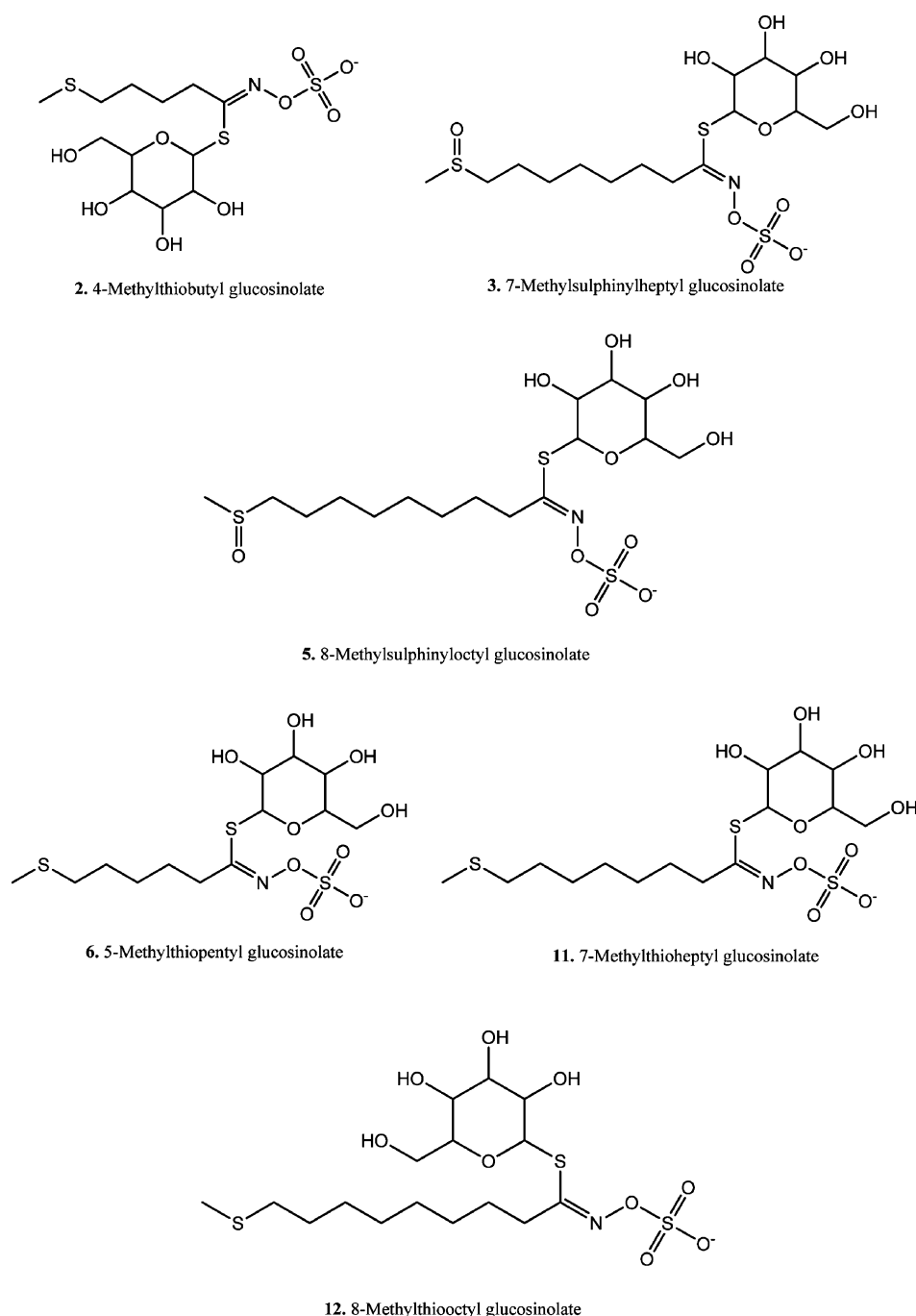


**Figure 2.** Structures of detected aliphatic glucosinolates.

265 min) saved in each analysis. Therefore, in the following  
 266 analyses, the short gradient was chosen along with the  
 267 ProntoSIL C18SH column.

268 **Identification of Glucosinolates and Camalexin in**  
 269 **Stressed *Arabidopsis* Mutants.** The capability of QTOF-MS  
 270 to measure masses with high accuracy makes this platform a  
 271 suitable tool to perform nontargeted analysis. Therefore,  
 272 characteristic fragmentation patterns allow the identification  
 273 of glucosinolates and camalexin with a high degree of  
 274 confidence without having to use pure standards. In the  
 275 present study, typical fragmentation patterns were used to  
 276 identify glucosinolates and camalexin. Moreover, the biological  
 277 information of *Arabidopsis* mutants (*pad3*, *pen3.1*, and  
 278 *cyp79B2/B3*) as well as Col-0 accessions contributed to the

279 unequivocal identification of the analytes considered in this  
 280 study. Ten glucosinolates, camalexin, and other related  
 281 compounds were identified (Table 1).

282 Compounds 4, 7, and 9 were annotated as indolic  
 283 glucosinolates, whereas compounds 2, 3, 5, 6, 11, and 12  
 284 (Table 1) were tentatively annotated as aliphatic glucosinolates.  
 285 On the basis of recent literature,<sup>19</sup> compound 10 was also  
 286 tentatively annotated as an aliphatic glucosinolate with seven  
 287 carbons in a linear or branched chain, the extent of which could  
 288 not be properly determined with mass spectrometry data. With  
 289 the chromatographic conditions used in this work, it was not  
 290 possible to properly retain other previously reported aliphatic  
 291 glucosinolates such as 3-methylsulfinylpropyl, 5-methylsulfinyl-  
 292 pentyl, and 6-methylsulfinylhexyl. However, the methodology

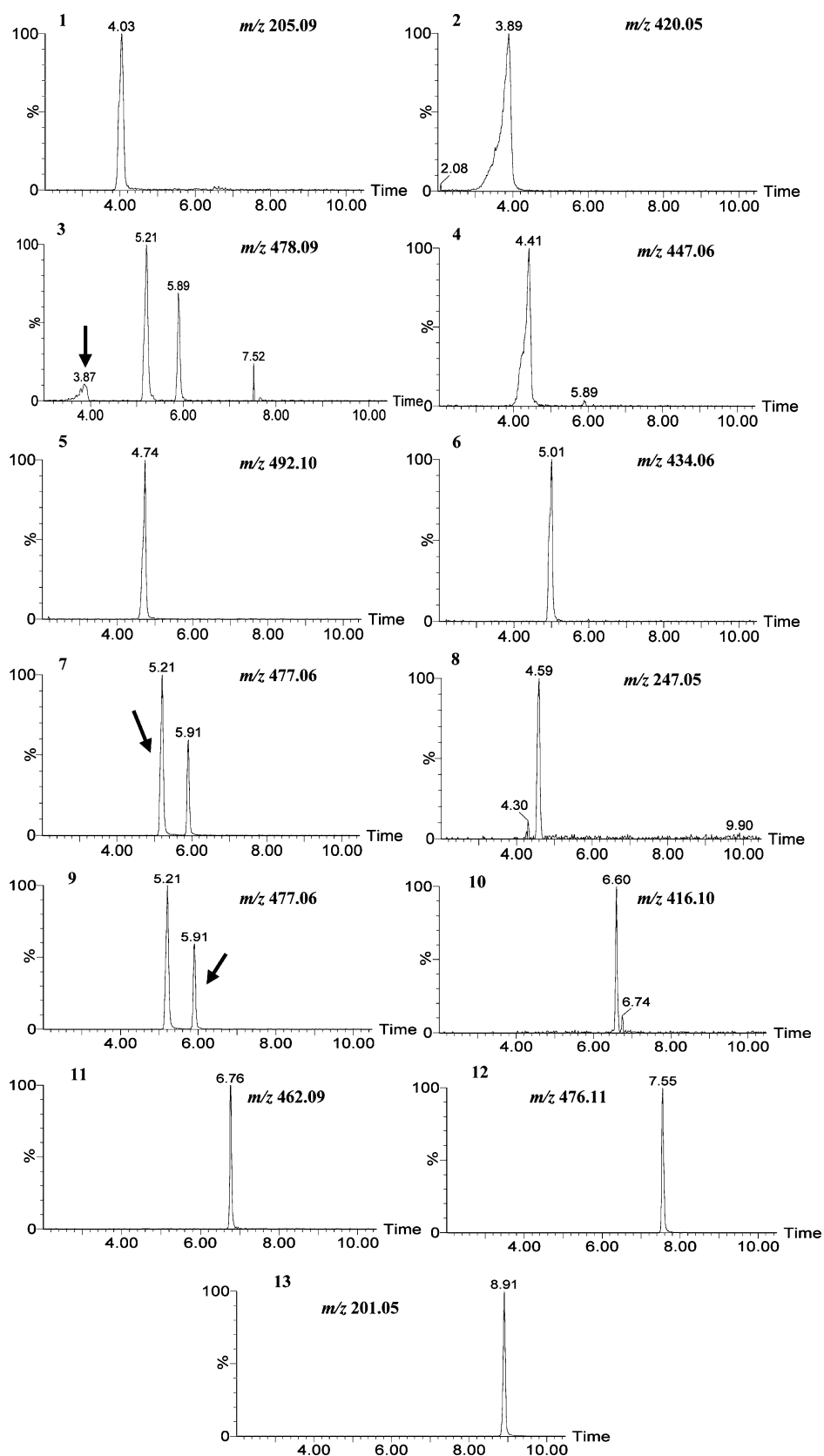


**Figure 3.** Extracted ion chromatograms for the 10 identified glucosinolates and camalexin. Values within each chromatogram represent  $m/z$  used for the extracted ion chromatogram.

proved to be sufficient to profile indolic glucosinolates. Related metabolites such as tryptophan (1) and dihydrocamalexin acid (8) were identified and annotated based on biological as well as

mass spectrometric data. Extracted ion chromatograms for each compound are shown in Figure 3. As observed in chromatograms, both compounds 7 and 9 showed a maximum at 477.06

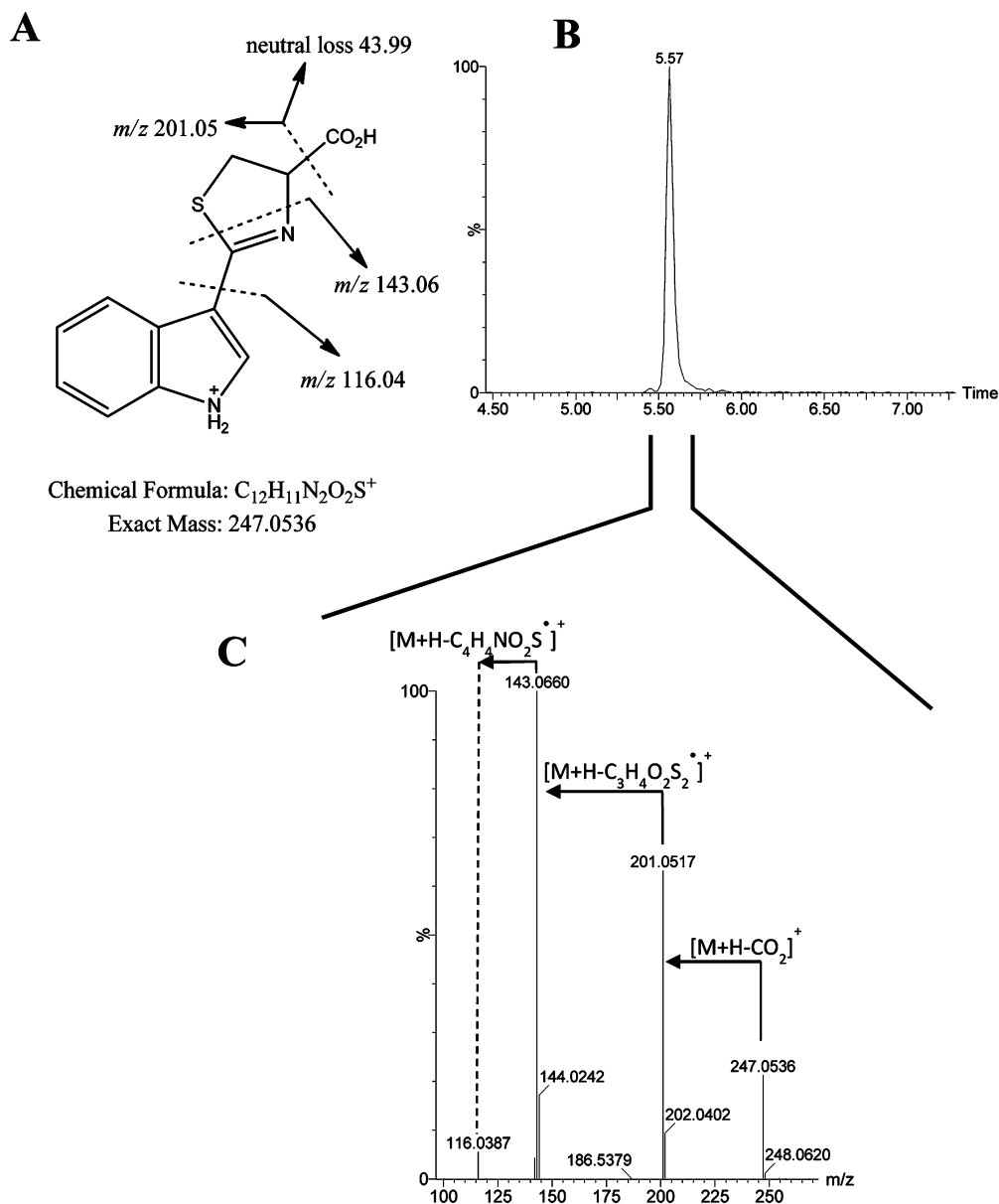


**Figure 4.** Identification of dihydrocamalexin by mass spectrometry: fragmentation pattern of dihydrocamalexin (A), chromatographic peak of dihydrocamalexin (B), and fragment ions observed upon collision-induced dissociation (C).

299 corresponding to the  $[M - H]^-$  of 4-methoxyindol-3-ylmethyl  
300 glucosinolate and the 1-methoxy isomer, respectively. Identifi-  
301 cation of each of the isomers was accomplished by their  
302 elution order.<sup>19</sup>

303 Characteristic fragmentation patterns were analyzed to  
304 confirm the identity of each compound. Table 1 shows the  
305 main fragments obtained from each extracted ion chromato-  
306 gram from function 2 acquisition. The characteristic fragment  
307 peak at  $m/z$  96.96 was observed in all recorded glucosinolate  
308 spectra representing a bisulfate anion ( $\text{HSO}_4^-$ ) released after  
309 cleavage of intact glucosinolates. A chromatographic peak  
310 eluting at 2.0 min with a  $m/z$  of 463.05 compatible with the  
311 pseudomolecular ion ( $[M - H]^-$ ) from 4-hydroxyindol-3-  
312 ylmethyl glucosinolate was observed, although its identity could  
313 not be properly confirmed due to the low signal intensity  
314 shown that rendered a poor fragmentation in function 2.

315 To verify these results, leaf extracts of stressed *Arabidopsis*  
316 *cyp79B2/B3* plants were analyzed by mass spectrometry. The

*cyp79B2/B3* double mutant is a hybrid between two lines 317  
318 identified in a loss-of-function screening on a T-DNA insertion  
319 collection of the Col-0 ecotype. The T-DNA insertions disrupt  
320 their respective genes, rendering null alleles<sup>24</sup> and plants devoid  
321 in any indolic glucosinolate or camalexin.<sup>22</sup> In the original  
322 article,<sup>24</sup> the authors reported subtle phenotype differences  
323 between *cyp79B2/B3* double mutant and its respective wild-  
324 type Col-0; however, under the growth conditions used in this  
325 study, both sets of plants were completely indistinguishable  
326 (data not shown). As expected, indolic glucosinolates (4, 7, and  
327 9) were not detected in any of these samples, whereas aliphatic  
328 glucosinolates (2, 3, 5, 6, and 10–12) were detected in  
329 *cyp79B2/B3* extracts. *Arabidopsis pad3*, isolated from an  
330 ethylmethanesulfonate mutant population,<sup>23</sup> carries a single  
331 nucleotide deletion, leading to an early stop codon in the  
332 predicted open reading frame that originates truncated mRNA,  
333 which is not translated into a functional CYP71B15 enzyme  
334 (that converts dihydrocamalexin into camalexin). Corre-



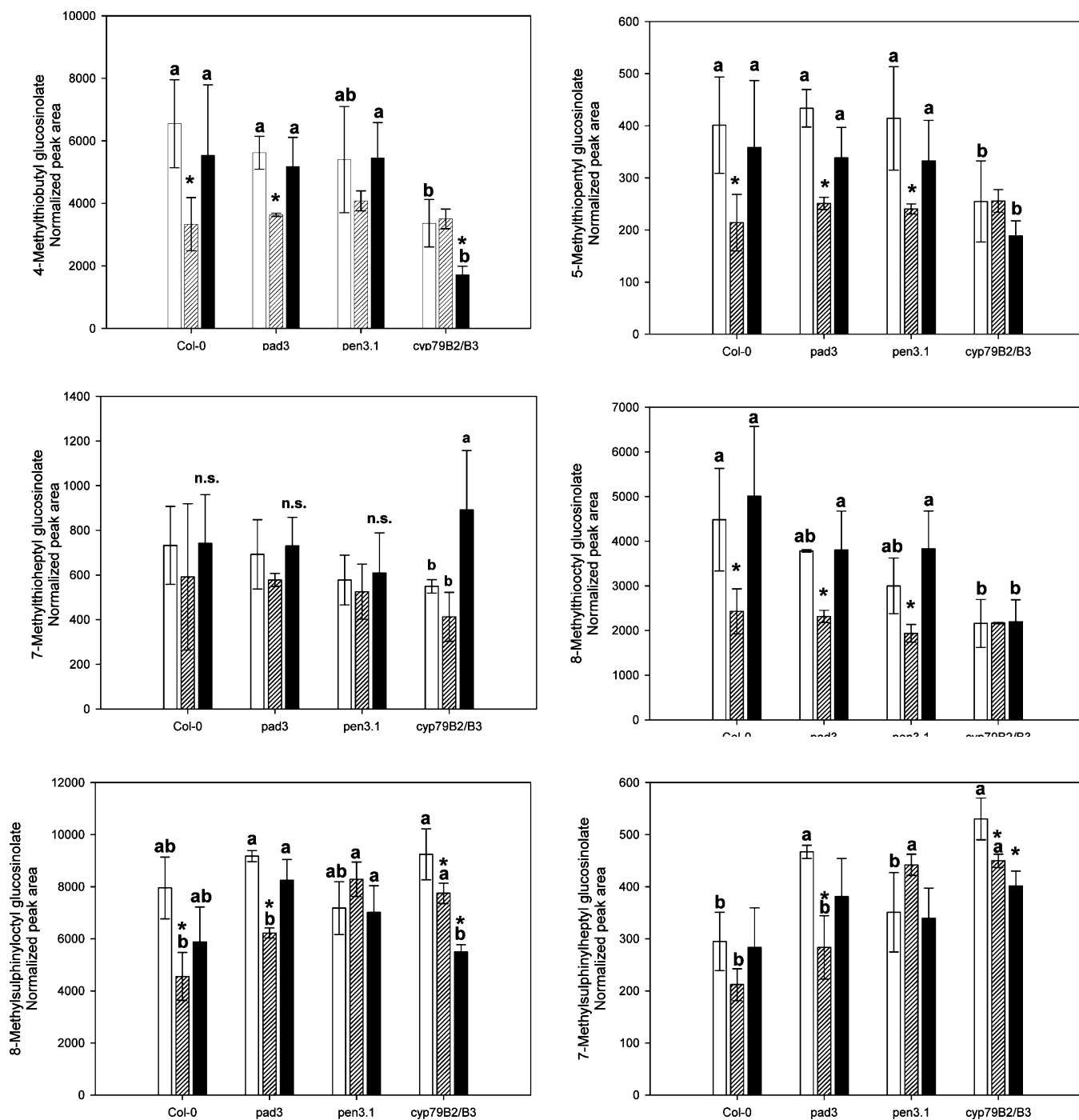


**Figure 5.** Relative quantitation of aliphatic glucosinolate levels in *Arabidopsis* rosette leaves in response to abiotic and biotic stresses. White bars represent control plants sprayed with tap water, striped bars represent plants sprayed with a *B. cinerea* conidia suspension, and black bars represent plants sprayed with a  $\text{AgNO}_3$  solution. Asterisks (\*) denote statistical significance at  $P \leq 0.05$  with controls. Different letters denote statistical differences among genotypes subjected to the same treatment at  $P \leq 0.05$ ; n.s., not significant.

spondingly, camalexin could not be detected either in *pad3* or in *cyp79B2/B3* leaf extracts. Nevertheless, a mass chromatographic feature showing a fragmentation pattern compatible with the presence of camalexin, an indolic ring, and neutral losses of  $\text{H}_2\text{CO}_2$  and  $\text{C}_3\text{H}_4\text{O}_2\text{S}$  was observed (Figure 4). This mass chromatographic feature was annotated as dihydrocamalexin acid, the immediate precursor of camalexin and substrate of phytoalexin-deficient-3 (PAD3) protein, by comparison with the reported data in the literature.<sup>22</sup> This metabolite was

strongly accumulated in *pad3* plants after stress imposition (Figure 6).

**Evaluation of the Stress Treatments.** The impact of abiotic and biotic stress treatments on the analytes described above was evaluated after LC/ESI-QTOF-MS analysis. The relative quantitation was carried out first by determining recovery of the internal standard biochanin A (Table 1) to correct areas of target analytes. Finally, corrected peak areas were normalized to the amount of tissue used. Figure 5 shows

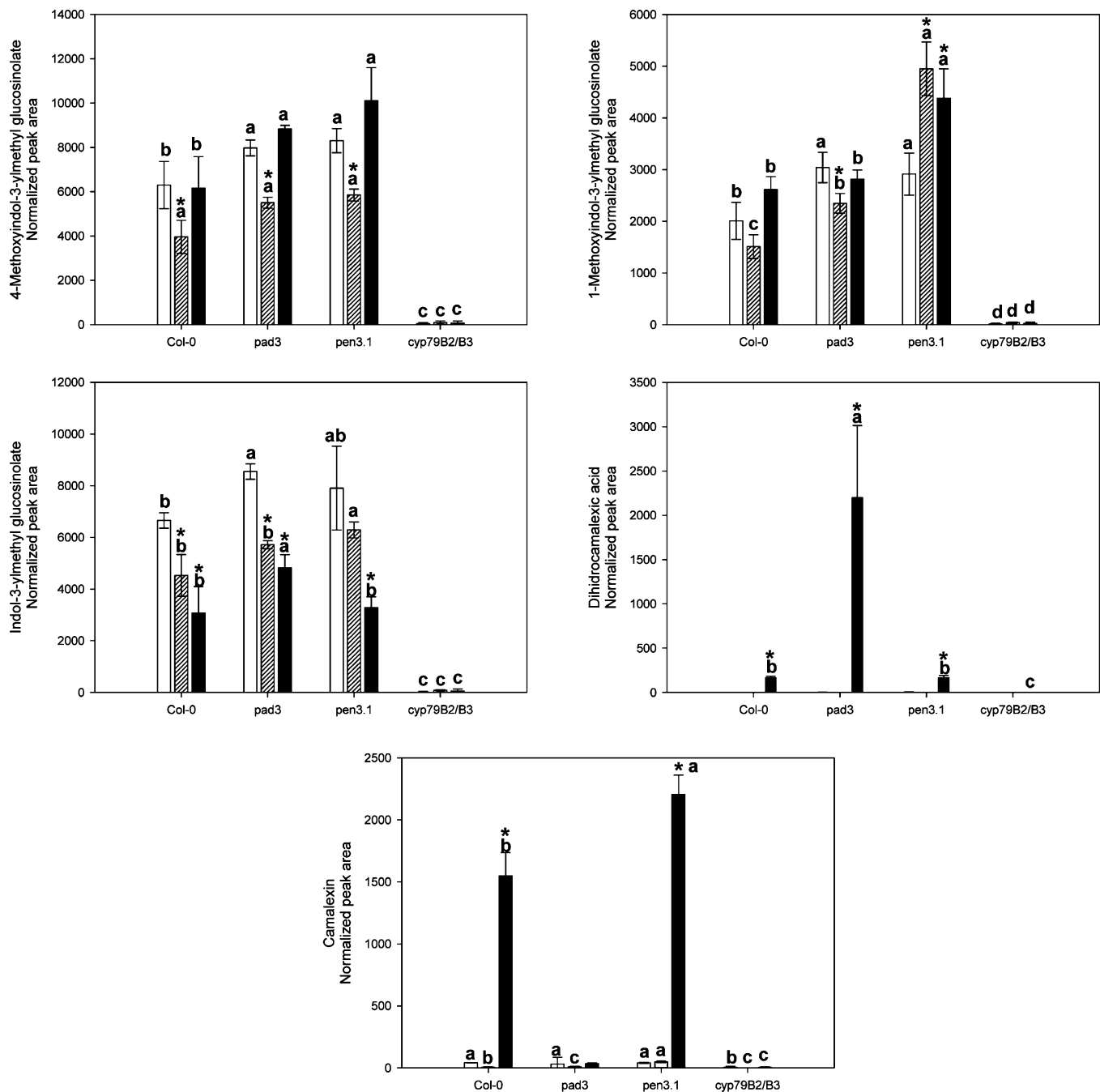


**Figure 6.** Relative quantification of indolic glucosinolates, dihydrocamalexin acid and camalexin levels in *Arabidopsis* rosette leaves in response to abiotic and biotic stresses. White bars represent control plants sprayed with tap water, striped bars represent plants sprayed with a *B. cinerea* conidia suspension, and black bars represent plants sprayed with a  $AgNO_3$  solution. Asterisks (\*) denote statistical significance at  $P \leq 0.05$  with controls. Different letters denote statistical differences among genotypes subjected to the same treatment at  $P \leq 0.05$ .

353 aliphatic glucosinolate concentrations in the different genotypes  
354 under control and stress conditions.

355 First, it should be noted that the different mutations had an  
356 effect on basal aliphatic glucosinolate levels. In general,  
357 *cyp79B2/B3* showed much reduced levels of aliphatics (over  
358 50% for 2 and 12 and 40% for 6). Nevertheless, both *pad3* and  
359 *cyp79B2/B3* showed higher basal levels of 3, with respect to  
360 Col-0. Spraying *Arabidopsis* plants with a *Botrytis* conidia  
361 suspension reduced below control levels most aliphatic  
362 glucosinolates such as 2, 6, 5, 12, and 3 in Col-0 and *pad3*.  
363 The mutant *pen 3.1*, highly sensitive to biotic stress [*PEN3*  
364 encodes for an ATP binding cassette (ABC) transporter

involved in the targeted export of toxins to penetration sites], 365  
366 exhibited a slightly different trend, since treatment with the  
367 fungus conidia increased 5 and 3 levels. In the double mutant,  
368 *cyp79B2/B3*, a different trend for 2, 6, and 12 was also observed  
369 with no significant differences with controls in response to the  
370 biotic elicitor. Levels of aliphatic glucosinolates did not  
371 significantly vary in *Arabidopsis* plants treated with  $AgNO_3$   
372 solution except in the case of *cyp79B2/B3* mutants. In this  
373 genotype, abiotic stress reduced levels of 2, 6, 5, and 3 and  
374 increased the concentration of 11.

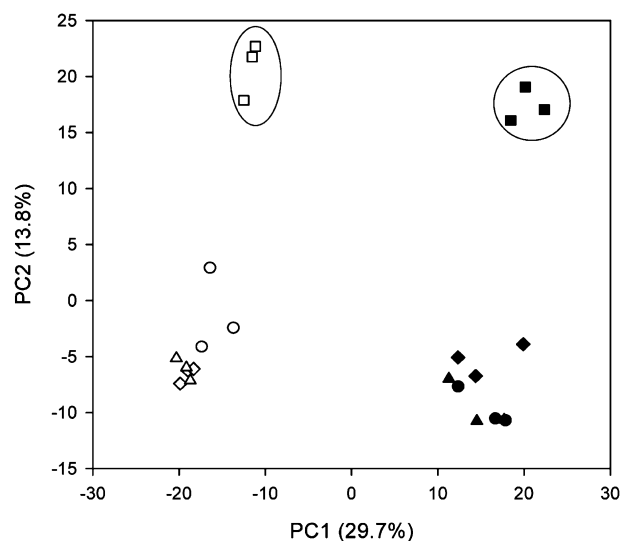
Basal levels of indolic glucosinolates (Figure 6) were 375  
376 significantly higher in *pad3* and *pen 3.1*. This could be likely

377 a feedback response to the constitutive absence of camalexin. In  
 378 addition, an expected result was the complete absence of these  
 379 metabolites in the *cyp79B2/B3* mutant as it is impaired in the  
 380 activity that catalyzes the conversion of tryptophan to indolic-3-  
 381 acetaldoxime (Figure 1). In addition, compounds 13 and 8  
 382 were absent in these plants after treatment with AgNO<sub>3</sub> or  
 383 *Botrytis*. Moreover, also as predicted, *pad3* mutant failed to  
 384 accumulate camalexin (13) upon stress treatment but over-  
 385 accumulated dihydrocamalexic acid (8), the immediate  
 386 metabolic precursor of camalexin.<sup>28</sup> In general, treatment  
 387 with *Botrytis* conidia suspension reduced all indolic glucosino-  
 388 lates analyzed in Col-0 and *pad3*, whereas spraying with AgNO<sub>3</sub>  
 389 did not change their levels with respect to controls. On the  
 390 contrary, in *pen 3.1* plants, levels of 9 increased in response to  
 391 biotic or abiotic elicitors with respect to controls, reflecting its  
 392 higher sensitivity to both kinds of adverse conditions.<sup>20</sup> Levels  
 393 of compound 13 significantly increased upon spraying with  
 394 AgNO<sub>3</sub> solution in Col-0 and *pen 3.1* mutants, but they did not  
 395 vary in response to *Botrytis* treatment. In addition, this  
 396 metabolite could not be observed in *pad3* or *cyp79B2/B3*  
 397 mutants. As expected, the dihydrocamalexic acid (8) concen-  
 398 tration increased in AgNO<sub>3</sub>-treated *pad3* plants instead (2000-  
 399 fold with respect to control values) and to a much lower extent  
 400 in Col-0 and *pen 3.1*, directly linking camalexin (13) production  
 401 to the previous accumulation of dihydrocamalexic acid (8).

402 It has been shown that inoculation of *A. thaliana* with *B.*  
 403 *cinerea* conidia reduces both aliphatic and indolic glucosinolate  
 404 contents.<sup>29</sup> However, the apparent inconsistency of our data  
 405 with previous reports showing that *B. cinerea*, a necrotrophic  
 406 ascomycete, induces camalexin production and accumulation in  
 407 *Arabidopsis* can be partially explained by the fact that some *B.*  
 408 *cinerea* isolates are camalexin-tolerant and capable of detoxify-  
 409 ing this phytoalexin.<sup>29</sup>

410 **Differences among *Arabidopsis* Mutants under Con-**  
 411 **trol Conditions.** The complete data set of each *Arabidopsis*  
 412 genotype was analyzed by PCA (Figure 7). The first two  
 413 principal components explained 43.6% of the total variance in  
 414 negative mode and 53.0% in positive mode. As extracted from  
 415 the PCA plots, principal component 1 (PC1) explained the  
 416 experimental variation associated with this kind of experiment  
 417 and clearly differentiated the two biological replicates, whereas  
 418 PC2 was associated with genotype-specific variation. Hence,  
 419 PC2 clearly discriminated Col-0, *pad3*, and *pen3.1* genotypes  
 420 from the *cyp79B2/B3* genotype. The similarity among Col-0,  
 421 *pad3*, and *pen3.1* genotypes allowed us to conclude that the  
 422 metabolic differences found among these genotypes only  
 423 appeared after stress imposition. On the contrary, clear basal  
 424 differences were found between any genotype and the double  
 425 mutant *cyp79B2/B3*. This genotype carries insertions in the  
 426 genes coding for the enzymes that catalyze the conversion of  
 427 tryptophan to indole-3-acetaldoxime, the first metabolite in the  
 428 indolic glucosinolates biosynthetic pathway, which also acts as a  
 429 precursor for camalexin biosynthesis.<sup>30</sup> To find out which  
 430 variables (metabolites) were behind these basal differences, a  
 431 PLS-DA analysis was performed. Among these variables, it was  
 432 found that indolic glucosinolates were important because they  
 433 were absolutely absent in *cyp79B2/B3* samples, as expected.  
 434 Strikingly, tryptophan (1) was also found to be important in  
 435 defining these differences. Relative quantitation of 1 in control  
 436 *cyp79B2/B3* was conducted and expressed in Figure 8. The  
 437 results obtained suggested that as a result of the metabolic  
 438 deficiency in cytochromes 79B2 and 79B3, the precursor  
 439 metabolite tryptophan (1) showed an accumulation of 4-fold

## A. Negative ionization mode



## B. Positive ionization mode

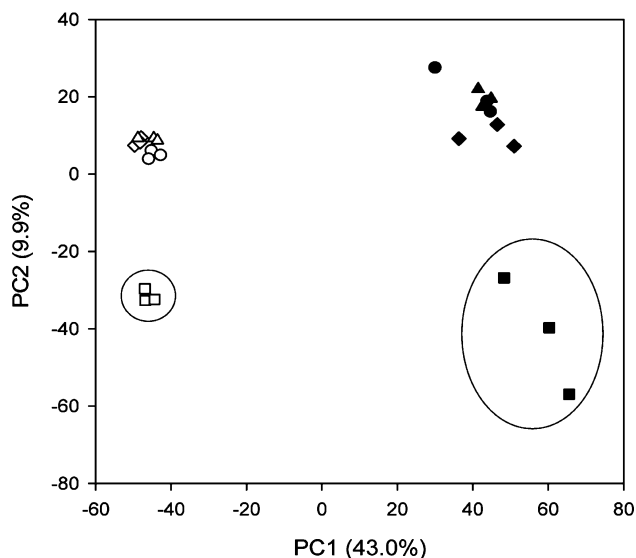


**Figure 7.** PCA of data sets belonging to *Arabidopsis* Col-0 (wild type) and *cyp79B2/B3*, *pad3*, and *pen3.1* mutant leaf extracts under control conditions. Plots represent the PCA analysis in negative (A) and positive (B) ionization modes. Symbols in black and white belong to *Arabidopsis* accessions in replicates 1 and 2, respectively. Refer to Col-0 (○), *cyp79B2/B3* (□), *pad3* (◇), and *pen3.1* (△). Circles indicate *cyp79B2/B3* sample groups in both negative and positive modes and in the two biological replicates.

with respect to the rest of genotypes included in this study. 440  
 These results also suggested that no negative feedback 441  
 mechanism prevented tryptophan from accumulating in leaf 442  
 rosettes of *cyp79B2/B3* plants. In addition, no specific 443  
 phenotype was observed (data not shown): leaf rosette and 444  
 inflorescence phenotype as well as development were identical 445  
 to that of Col-0 wild type, indicating that tryptophan 446  
 overaccumulation had no negative effects on plant perform- 447  
 ance.<sup>24</sup> 448

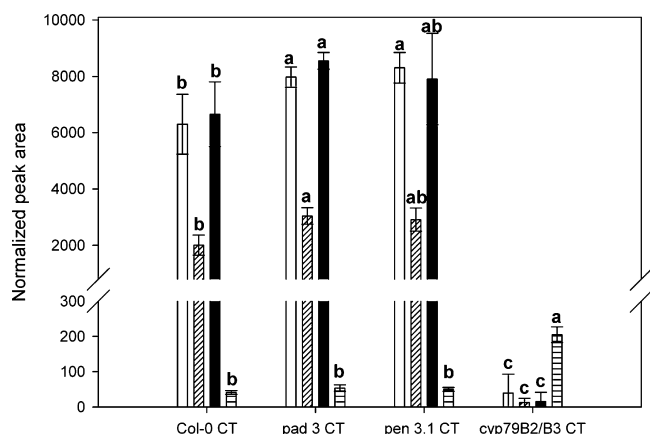


**Figure 8.** Relative quantitation of tryptophan and indolic glucosinolate levels in *Arabidopsis* rosette leaves under control conditions. White bars represent compound 7 levels, bars with diagonal lines represent compound 9 levels, black bars represent compound 4 levels, and bars with horizontal lines represent compound 1 levels. Different letters denote statistical differences among genotypes subjected to the same treatment at  $P \leq 0.05$ .

Overall, data presented in this work confirm the use of reversed phase liquid chromatography coupled to QTOF-MS as a useful methodology to profile semipolar compounds in plant extracts, especially glucosinolates and other defense-related compounds. In addition, the use of mutants carrying alterations in certain biosynthetic pathways in combination with mass spectrometry could be useful in the unequivocal identification of compounds for which commercial standards are unavailable. Both the inoculation with *B. cinerea* conidia and the treatment with a  $\text{AgNO}_3$  solution have an effect on secondary metabolism but not in the same direction, whereas the biotic elicitor depresses glucosinolate content without any direct effect on camalexin production, the abiotic stress treatment does not alter aliphatic or indolic glucosinolate contents but induces the accumulation of the phytoalexin camalexin. In addition, the impairment in PEN3 (PDR8) ATP-binding cassette transporter in the mutant *pen 3.1* has a positive effect on indolic glucosinolate and camalexin contents in response to biotic or abiotic elicitation and even in nonstressed plants, pointing out to the higher sensitivity of this genotype to stress. Finally, the impairment in cytochrome P79 enzyme activity seems to induce specific alterations in secondary metabolite composition even under nonstressful condition (such as the accumulation of tryptophan). Therefore, because the basal metabolic configuration is different to Col-0, their comparison in genetic and physiological studies should be taken with caution.

## ASSOCIATED CONTENT

### Supporting Information

Table of chromatographic columns tested and characteristics and number of peaks collected in the two gradients used and figure of total ion current chromatograms of plant extracts for the different columns and gradients assayed in this study. This material is available free of charge via the Internet at <http://pubs.acs.org>.

## AUTHOR INFORMATION

### Corresponding Author

\*Tel: +34 964 72 8101. Fax: +34 964 72 8216. E-mail: vicente.arbona@camn.uji.es.

### Funding

This work was supported by the Spanish Ministerio de Economía y Competitividad (MINECO) and Universitat Jaume I/Fundació Bancaixa through Grant Nos. AGL2010-22195-C03-01/AGR and P11B2009-01, respectively. V.A. was the recipient of a "Ramón y Cajal" contract from the MINECO.

### Notes

The authors declare no competing financial interest.

## ACKNOWLEDGMENTS

Seeds of *cyp79B2/B3*, *pad3*, and *pen 3.1* mutants were a kind gift of Christoph Böttcher from the Leibniz-Institut für Pflanzenbiochemie (Halle/Salle). Mass spectrometry analyses were performed at the central facilities (Servei Central d'Instrumentació Científica, SCIC) of Universitat Jaume I.

## ABBREVIATIONS USED

PCA, principal component analysis; PLS-DA, partial least-squares discriminant analysis

## REFERENCES

- (1) Avin-Wittenberg, T.; Tzin, V.; Angelovici, R.; Less, H.; Galili, G. Deciphering energy-associated gene networks operating in the response of *Arabidopsis* plants to stress and nutritional cues. *Plant J.* **2012**, *70*, 954–966.
- (2) Lehmann, M.; Laxa, M.; Sweetlove, L. J.; Fernie, A. R.; Obata, T. Metabolic recovery of *Arabidopsis thaliana* roots following cessation of oxidative stress. *Metabolomics* **2012**, *8*, 143–153.
- (3) Arbona, V.; Marco, A. J.; Iglesias, D. J.; Lopez-Climent, M. F.; Talon, M.; Gomez-Cadenas, A. Carbohydrate depletion in roots and leaves of salt-stressed potted *Citrus clementina* L. *Plant Growth Regul.* **2005**, *46*, 153–160.
- (4) Arbona, V.; Argamasilla, R.; Gómez-Cadenas, A. Common and divergent physiological, hormonal and metabolic responses of *Arabidopsis thaliana* and *Thellungiella halophila* to water and salt stress. *J. Plant Physiol.* **2010**, *167*, 1342–1350.
- (5) Schenke, D.; Böttcher, C.; Scheel, D. Crosstalk between abiotic ultraviolet-B stress and biotic (flg22) stress signalling in *Arabidopsis* prevents flavonol accumulation in favor of pathogen defence compound production. *Plant Cell Environ.* **2011**, *34*, 1849–1864.
- (6) Ahuja, I.; Kissen, R.; Bones, A. M. Phytoalexins in defense against pathogens. *Trends Plant Sci.* **2012**, *17*, 73–90.
- (7) Kerchev, P. I.; Fenton, B.; Foyer, C. H.; Hancock, R. D. Plant responses to insect herbivory: Interactions between photosynthesis, reactive oxygen species and hormonal signalling pathways. *Plant Cell Environ.* **2012**, *35*, 441–453.
- (8) Pollastri, S.; Tattini, M. Flavonols: Old compounds for old roles. *Ann. Bot.* **2011**, *108*, 1225–1233.
- (9) Arbona, V.; Iglesias, D. J.; Talón, M.; Gómez-Cadenas, A. Plant phenotype demarcation using nontargeted LC-MS and GC-MS metabolite profiling. *J. Agric. Food Chem.* **2009**, *57*, 7338–7347.
- (10) Agerbirk, N.; De Vos, M.; Kim, J. H.; Jander, G. Indole glucosinolate breakdown and its biological effects. *Phytochem. Rev.* **2009**, *8*, 101–120.
- (11) Malitsky, S.; Blum, E.; Less, H.; Venger, I.; Elbaz, M.; Morin, S.; Eshed, Y.; Aharoni, A. The transcript and metabolite networks affected by the two clades of *Arabidopsis* glucosinolate biosynthesis regulators. *Plant Physiol.* **2008**, *148*, 2021–2049.
- (12) Grubb, C. D.; Abel, S. Glucosinolate metabolism and its control. *Trends Plant Sci.* **2006**, *11*, 89–100.



- 545 (13) Agerbirk, N.; Olsen, C. E.; Sørensen, H. Initial and final  
546 products, nitriles, and ascorbigenes produced in myrosinase-catalyzed  
547 hydrolysis of indole glucosinolates. *J. Agric. Food Chem.* **1998**, *46*,  
548 1563–1571.
- 549 (14) Brown, P. D.; Tokuhisa, J. G.; Reichelt, M.; Gershenzon, J.  
550 Variation of glucosinolate accumulation among different organs and  
551 developmental stages of *Arabidopsis thaliana*. *Phytochemistry* **2003**, *62*,  
552 471–481.
- 553 (15) Kliebenstein, D. J.; Kroymann, J.; Brown, P.; Figuth, A.;  
554 Pedersen, D.; Gershenzon, J.; Mitchell-Olds, T. Genetic control of  
555 natural variation in *Arabidopsis* glucosinolate accumulation. *Plant*  
556 *Physiol.* **2001**, *126*, 811–825.
- 557 (16) Mewis, I.; Appel, H. M.; Hom, A.; Raina, R.; Schultz, J. C. Major  
558 signaling pathways modulate *Arabidopsis thaliana* (L.) glucosinolate  
559 accumulation and response to both phloem feeding and chewing  
560 insects. *Plant Physiol.* **2005**, *138*, 1149–1162.
- 561 (17) Kim, J. H.; Jander, G. *Myzus persicae* (green peach aphid)  
562 feeding on *Arabidopsis* induces the formation of a deterrent indole  
563 glucosinolate. *Plant J.* **2007**, *49*, 1008–1019.
- 564 (18) Von Roepenack-Lahaye, E.; Degenkolb, T.; Zerjeski, M.; Franz,  
565 M.; Roth, U.; Wessjohann, L.; Schmidt, J.; Scheel, D.; Clemens, S.  
566 Profiling of *Arabidopsis* secondary metabolites by capillary liquid  
567 chromatography coupled to electrospray ionization quadrupole time-  
568 of-flight mass spectrometry. *Plant Physiol.* **2004**, *134*, 548–559.
- 569 (19) Glauser, G.; Schweizer, F.; Turlings, T. C. J.; Reymond, P. Rapid  
570 profiling of intact glucosinolates in *Arabidopsis* leaves by UHPLC-  
571 QTOFMS using a charged surface hybrid column. *Phytochem. Anal.*  
572 **2012**, *23*, 520–528.
- 573 (20) Stein, M.; Dittgen, J.; Sánchez-Rodríguez, C.; Hou, B.; Molina,  
574 A.; Schulze-Lefert, P.; Lipka, V.; Somerville, S. C. *Arabidopsis* PEN3/  
575 PDR8, an ATP binding cassette transporter, contributes to nonhost  
576 resistance to inappropriate pathogens that enter by direct penetration.  
577 *Plant Cell.* **2006**, *18*, 731–746.
- 578 (21) Tsuji, J.; Zook, M.; Somerville, S. C.; Last, R. L.;  
579 Hammerschmidt, R. Evidence that tryptophan is not a direct  
580 biosynthetic intermediate of camalexin in *Arabidopsis thaliana*. *Physiol.*  
581 *Mol. Plant Pathol.* **1993**, *43*, 221–229.
- 582 (22) Böttcher, C.; Westphal, L.; Schmotz, C.; Prade, E.; Scheel, D.;  
583 Glawischnig, E. The multifunctional enzyme CYP71B15 (PHYTOA-  
584 LEXIN DEFICIENT3) converts cysteine-indole-3-acetonitrile to  
585 camalexin in the indole-3-acetonitrile metabolic network of *Arabidopsis*  
586 *thaliana*. *Plant Cell.* **2009**, *21*, 1830–1845.
- 587 (23) Glazebrook, J.; Ausubel, F. M. Isolation of phytoalexin-deficient  
588 mutants of *Arabidopsis thaliana* and characterization of their  
589 interactions with bacterial pathogens. *Proc. Natl. Acad. Sci. U.S.A.*  
590 **1994**, *91*, 8955–8959.
- 591 (24) Zhao, Y.; Hull, A. K.; Gupta, N. R.; Goss, K. A.; Alonso, J.;  
592 Ecker, J. R.; Normanly, J.; Chory, J.; Celenza, J. L. Trp-dependent  
593 auxin biosynthesis in *Arabidopsis*: Involvement of cytochrome P450s  
594 CYP79B2 and CYP79B3. *Genes Dev.* **2002**, *16*, 3100–3112.
- 595 (25) Muckenschnabel, I.; Goodman, B. A.; Williamson, B.; Lyon, G.  
596 D.; Deighton, N. Infection of leaves of *Arabidopsis thaliana* by *Botrytis*  
597 *cinerea*: Changes in ascorbic acid, free radicals and lipid peroxidation  
598 products. *J. Exp. Bot.* **2002**, *53*, 207–214.
- 599 (26) <http://metlin.scripps.edu/download/>.
- 600 (27) Ibañez, M.; Sancho, J. V.; Pozo, O. J.; Niessen, W.; Hernández,  
601 F. Use of liquid chromatography quadrupole time-of-flight mass  
602 spectrometry in the elucidation of transformation products and  
603 metabolites of pesticides. Diazinon as a case study. *Rap. Commun. Mass*  
604 *Spectrom.* **2006**, *384*, 169–178.
- 605 (28) Glawischnig, E. Camalexin. *Phytochemistry* **2007**, *68*, 401–406.
- 606 (29) Kliebenstein, D. J.; Rowe, H. C.; Denby, K. J. Secondary  
607 metabolites influence *Arabidopsis/Botrytis* interactions: Variation in  
608 host production and pathogen sensitivity. *Plant J.* **2005**, *44*, 25–36.
- 609 (30) Glawischnig, E.; Hansen, B. G.; Olsen, C. E.; Halkier, B. A.  
610 Camalexin is synthesized from indole-3-acetaldoxime, a key branching  
611 point between primary and secondary metabolism in *Arabidopsis*. *Proc.*  
612 *Natl. Acad. Sci. U.S.A.* **2004**, *101*, 8245–8250.